


Graphene-Based Magnetically Tunable Broadband Terahertz Absorber

Zhenyan Wei, Yannan Jiang , Member, IEEE, Shitian Zhang, Xiuqin Zhu, and Qingliang Li

Abstract—This study proposes a broadband absorber based on graphene and one-dimensional photonic crystal (1DPC) to achieve magnetically tunable broadband absorption in the terahertz (THz) frequency range. The performance is analyzed using the 4×4 transfer matrix method, demonstrating that the proposed absorber operates in a broadband range of 3.34 to 4.68 THz for left-handed circularly polarized (LCP) waves with an absorption greater than 90%. The localized THz wave produces absorption peaks, achieves broadband with high absorption, and is tuned dynamically by varying the magnetic field. This work has potential for many applications, such as broadband filters, anti-radar stealth, and sensors.

Index Terms—Broadband absorber, graphene, photonic crystals, magnetic tunable.

I. INTRODUCTION

GRAPHENE has unique properties, such as optical / terahertz (THz) absorption [1], [2] and tunable surface conductivity [3], [4]. It has been widely used in the investigation of absorbers for the realization of dynamically tunable absorption. Additionally, one-dimensional photonic crystal (1DPC) can be combined with graphene to efficiently improve the absorption performance due to its many advantages, such as simple structure, convenient preparation, and controllable optical transmission [5]. Initially, the photonic crystal was used to control optical transmission [6], [7]. Subsequently, most absorbers based on graphene and 1DPC operated in an optical range with narrowband [8], multi-band [9], and broadband [10] absorption.

THz waves have advantages such as wide bandwidth, robust transmission, and high resolution. As such, they have great potential in many fields, such as communication [11], imaging [12], and biomedicine [13]. The wide application of the THz wave is considerably related to detection, and the THz absorber

is a critical component for detecting THz waves [14]. Therefore, the combination of graphene and photonic crystals is utilized in THz absorbers to achieve multi-band [15], [16] and broadband [17] absorption. Up to now, graphene-based absorbers could be generally tuned by varying the Fermi level of the graphene. The main techniques for varying the Fermi level are chemical doping and an external bias electric field [18]. Chemical doping can be achieved by replacing the carbon atoms in graphene with other atoms or by adsorbing other molecules or atoms onto the graphene. Nevertheless, this technique is absent from dynamic tunability. An external bias electric field can dynamically tune the surface conductivity of graphene and the absorption of the graphene-based absorber. However, this drastically increases the difficulty of manufacturing. Furthermore, graphene can also be magnetized using a static bias magnetic field (SBMF) and dynamically tuned, thus the graphene-based absorber can be tuned accordingly. To the best of our knowledge, there are few reports on magnetically tunable THz absorbers. Crucially, this technique is non-contact and free of electrodes, which can effectively reduce the difficulty of manufacturing. Using the SBFM, Rashidi *et al.* investigated the circularly polarized wave absorption performance of a graphene-based 1DPC in the THz region [19]. However, this work was limited to narrowband absorption. Broadband absorption is more widely valuable for several components, such as sensors, modulators, and anti-reflection coatings [20].

In this study, a graphene-based 1DPC broadband absorber is proposed by tuning the SBFM. The proposed absorber consists of multiple elementary units, which are comprised of monolayer graphene and two periodic 1DPCs with a spacer layer. The 4×4 transfer matrix method is then employed to analyze the absorption performance. The results show that the proposed absorber can absorb the left-handed circularly polarized (LCP) wave from 3.34–4.68 THz (i.e., a relative bandwidth of 33.42%) with an absorption greater than 90%.

II. MODEL AND METHOD

A. Electric Parameter Model of Magnetized Graphene

Magnetized by a perpendicular SBFM, graphene has conductivity components with longitudinal conductivity σ_{xx} and Hall conductivity σ_{xy} , which can be described in the THz regime by the Drude model [21] and are respectively expressed as:

$$\sigma_{xx}(\omega, B) = \frac{D}{\pi} \frac{\Gamma - i\omega}{\omega_c^2 - (\omega + i\Gamma)^2} \quad (1)$$

Manuscript received October 25, 2021; revised November 26, 2021; accepted November 30, 2021. Date of publication December 6, 2021; date of current version December 27, 2021. This work was supported in part by the National Natural Science Foundation of China under Grant 61661012, in part by the Natural Science Foundation of Guangxi Province under Grants 2019GXNSFFA245002 and 2018GXNSFAA281190, in part by the Key Laboratories for National Defense Science and Technology under Grant 202003007, in part by the Dean Project of Guangxi Key Laboratory of Wireless Wideband Communication and Signal Processing under Grants GXKL06180108, GXKL06190114, GXKL06190118, and GXKL06200127, and in part by the Middle-aged and Young Teachers' Basic Ability Promotion Project of Guangxi under Grant 2020KY05028. (Corresponding author: Yannan Jiang.)

Zhenyan Wei and Yannan Jiang are with the Guangxi Key Laboratory of Wireless Wideband Communication & Signal Processing, Guilin 541004, China (e-mail: zywei@guet.edu.cn; ynjjiang@guet.edu.cn).

Shitian Zhang, Xiuqin Zhu, and Qingliang Li are with the National Key Laboratory of Electromagnetic Environment, Qingdao 266107, China (e-mail: shitian_zhang@126.com; xiuqin_zhu@sohu.com; qlianglicirp@sina.cn).

Digital Object Identifier 10.1109/JPHOT.2021.3132795

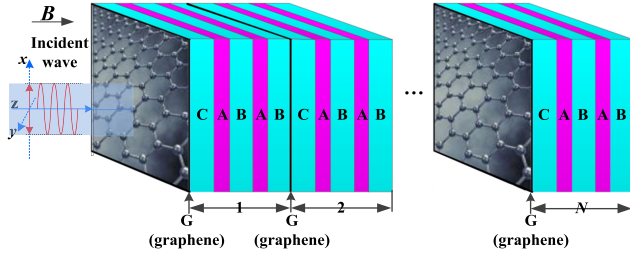


Fig. 1. Schematic representation of the proposed $(GC(AB)^M)^N$ model.

and

$$\sigma_{xy}(\omega, B) = -\frac{D}{\pi} \frac{\omega_c}{\omega_c^2 - (\omega + i\Gamma)^2} \quad (2)$$

where $D = e^2|E_F|/\hbar^2$ is the Drude weight and $\omega_c = eBv_F^2/E_F$ is the cyclotron frequency. e , E_F , \hbar , v_F , and Γ are the electron charge, Fermi level, reduced Planck's constant, Fermi velocity, and scattering rate, respectively. The relative permittivity of graphene can be written as:

$$\vec{\epsilon}_g = \begin{pmatrix} \epsilon_{xx} & \epsilon_{xy} & 0 \\ -\epsilon_{xy} & \epsilon_{xx} & 0 \\ 0 & 0 & \epsilon_{zz} \end{pmatrix} \quad (3)$$

Here, $\epsilon_{xx} = 1 + i\sigma_{xx}/\omega\epsilon_0d_g$, $\epsilon_{xy} = i\sigma_{xy}/\omega\epsilon_0d_g$, and $\epsilon_{zz} = 1$, where ω , ϵ_0 , and d_g are the operating angular frequency, vacuum permittivity, and thickness of the graphene, respectively.

B. Absorber Model and Analytic Method

The proposed schematic model magnetized by the SBMF is shown in Fig. 1. This model can be described as $(GC(AB)^M)^N$, where G represents graphene, and A (magenta) and B (bright - blue) represent two nonmagnetic dielectrics with high and low refractive indexes, respectively. Furthermore, A and B form 1DPC. C (bright - blue) represents the spacer layer between the graphene and 1DPC, M is the period number of 1DPC, and $GC(AB)^M$ represents the elementary unit. Hence, N is the number of elementary units. In other words, the proposed model is formed by the cascading connection of N elementary units. The THz wave is normally incident on the structure, and the SBMF is along the same direction.

The transfer matrix method can be used to analyze the propagation in layered dielectric media [22], and the 4×4 transfer matrix method [23] is beneficial for the analysis of the wave response (reflectance, transmittance, and absorption) for right-handed circularly polarized (RCP) and LCP waves. This method was used to calculate the absorption of the proposed model $A^\pm = 1 - R^\pm - T^\pm$, where “+” and “-” represent the RCP and LCP waves, respectively.

III. RESULTS AND DISCUSSION

A. Absorption Performance of an Elementary Unit

First, the absorption performance of an elementary unit was analyzed to investigate the physical mechanism of the proposed model. In the elementary unit, A was set as SiO_2 with a dielectric

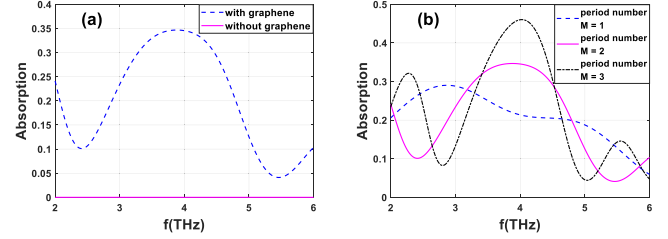


Fig. 2. Absorption of $B = 0$ T for: (a) $(GC(AB)^2)$ and $(C(AB)^2)$, and (b) $(GC(AB)^M)$. $M = 1, 2$, and 3 .

constants ϵ_A of 3.9 [24], and B and C were set as MgF_2 with $\epsilon_B = \epsilon_C = 1.9$ [25], [26]. In addition, the linearly polarized THz wave, with a central frequency f_0 of 3.9 THz, was normally incident on the proposed model. Moreover, the optical thicknesses of A , B , and C were a quarter of the central wavelength, that is, $\sqrt{\epsilon_A}d_A = \sqrt{\epsilon_B}d_B = \sqrt{\epsilon_C}d_C = \lambda_0/4$ (λ_0 is the wavelength in vacuum of f_0). In addition, the parameters of the graphene were $E_F = -0.34$ eV, $\Gamma = 10$ meV/ \hbar , $v_F = 10^6$ m/s, and $d_g = 0.335$ nm [27].

The absorptions of the elementary unit without graphene and with $B = 0$ T graphene are shown in Fig. 2(a). Here, the elementary unit without graphene did not achieve absorption because all dielectrics of the structure were lossless and no resonance of any form was presented. In contrast, the defect layer of 1DPC for the elementary unit with graphene, formed by the graphene G and spacer layer C , could localize the THz wave and produce the defect mode. Subsequently, the light-matter interaction between the localized waves and graphene were enhanced, which therefore increased the absorption of the elementary unit by approximately 30% in the 3.29 to 4.46 THz frequency range. Despite this, it can easily be determined from Fig. 2(a) that the absorption of an elementary unit was far less than 90%. This can be enhanced using three approaches [28]: 1) increasing the quality (Q) factor of the optical microcavity at the surface of the 1DPC, where the optical microcavity is composed of a graphene layer, spacer layer, and 1DPC (i.e., graphene and 1DPC act as the cavity mirrors and the spacer acts as the cavity); 2) increasing the absorption of the incident wave on the graphene; and 3) increasing the reflectance of the reciprocating waves in the optical microcavity.

Using the first approach, the Q factor of an elementary unit will be increased. However, this causes a narrowed absorption bandwidth. In the elementary unit, M can change the Q factor and they are proportional to one another, which can improve the absorption, as shown in Fig. 2(b). The bandwidth was enhanced and the absorption degraded when M decreased. Parenthetically, multiple elementary units were employed to enhance the absorption, as discussed in Section B. If the absorption of the elementary unit is too low or high, it will cause a large number of N or the absence of broadband, respectively. In other words, M is very important to the absorption and bandwidth.

The second and third approaches enhanced the absorption of the elementary unit by increasing the reflectance and absorption of THz waves on graphene, respectively. This can be achieved by increasing the thickness of the graphene [28]. However, this

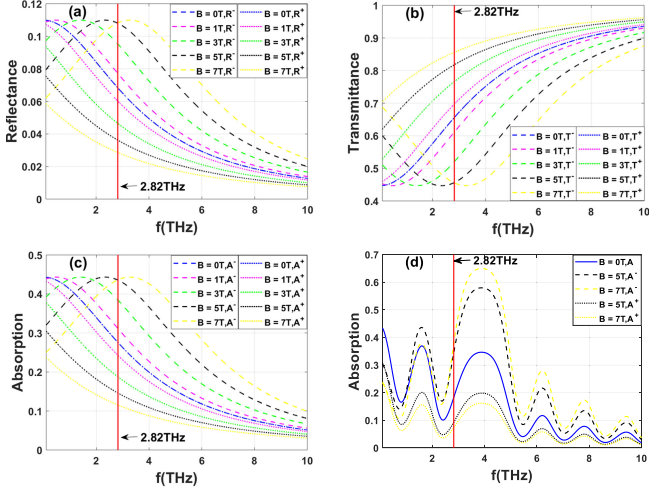


Fig. 3. Transmission and absorption of RCP (+) and LCP (-) waves with various SBMFs. (a) reflectance, (b) transmittance, (c) absorption of monolayer graphene, and (d) absorption of an elementary unit in the air.

achievement is limited by the absence of dynamic tunability. By varying the SBMF, the reflectance and absorption can be tuned, and dynamic tunability can be achieved. Furthermore, because of any linearly polarized wave that can be decomposed into two circularly polarized waves with opposite rotation directions (i.e., RCP and LCP waves), the responses of the RCP and LCP waves are investigated using various SBMFs.

The reflectance, transmittance, and absorption of monolayer graphene with various SBMFs for RCP (“+”) and LCP (“-”) waves were different due to the magnetic circular dichroism of the graphene [29], as shown in Figs. 3(a)–(c). The reflectance and absorption of the LCP / RCP waves increased / decreased in the frequency range of greater than 2.82 THz as the SBMF increased, as shown in Figs. 3(a) and (c), respectively. According to the second and third approaches, one can predict that the absorption of an elementary unit would behave the same, as shown in Fig. 3(d). Specifically, as the SBMF increased, the absorption of the LCP / RCP wave increased / decreased when the frequency range was greater than 2.82 THz. There was a larger absorption peak at a frequency of approximately 3.9 THz. In contrast, a frequency less than 2.82 THz demonstrated a nonidentical trend due to the ruleless reflectance and absorption of the LCP. Based on previous analyses, the proposed structure was investigated at approximately 3.9 THz.

B. Absorption Performance of Cascaded Elementary Units

Although the performance of an elementary unit can be enhanced by tuning the SBMF, the absorption is only approximately 0.65, as shown in Fig. 3(d). Therefore, cascaded elementary units are proposed to enhance absorption further.

1) *Cascaded Double Elementary Units*: First, the performance of cascaded double elementary units was investigated. The absorption of $(GC(AB)^1)^2$, $(GC(AB)^2)^2$, $(GC(AB)^3)^2$, and $(GC(AB)^1)^1(GC(AB)^3)^1$ for the THz wave at $B = 0$ T is shown in Fig. 4. Compared with Figs. 2(a) and 4, it is clear that

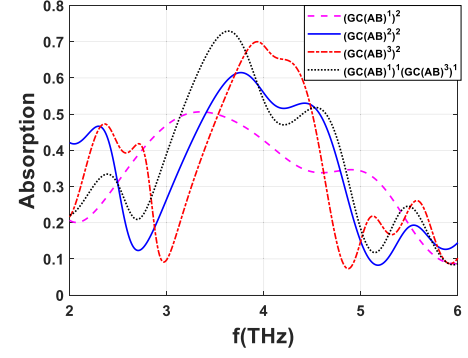


Fig. 4. Absorption of various cascaded double elementary units with $B = 0$ T.

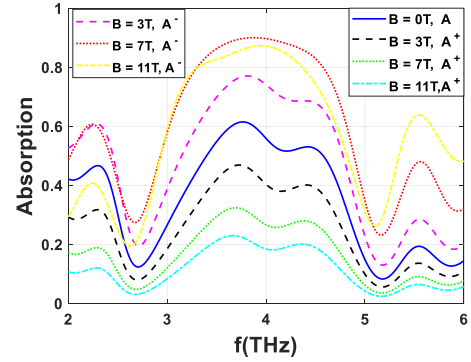


Fig. 5. Absorption of $(GC(AB)^2)^2$ for RCP (“+”) and LCP (“-”) waves for $B = 0, 3, 7,$ and 11 T.

the absorption of cascaded double elementary units was enhanced. This is because the defect layers (GC) could be mutually coupled through the evanescent field when M was small ($M \leq 4$), which is similar to that in coupled resonator optical waveguide structures [10]. This implies that the coupling is weak [30] and the absorption of cascaded double elementary units is dependent on the total absorption of the two single elementary units. The bandwidth of cascaded double elementary units presented a narrowed tendency as M increased, as shown in Fig. 4. This is because the increase of M weakened the interaction between the localized waves [31]. Furthermore, the absorption of $(GC(AB)^1)^1(GC(AB)^3)^1$ fluctuated significantly because of the different M in the two elementary units, which impeded the realization of broadband operation. Through the aforementioned comprehensive analysis, the optimal M was set to 2 in this study.

The tunable absorption of the cascaded double elementary unit $(GC(AB)^2)^2$ with various SBMFs was analyzed, demonstrating that the absorption of the LCP wave firstly increased and then decreased by increasing SBMF, as shown in Fig. 5. Moreover, $B = 7$ T achieved optimal absorption. However, the broadband absorption was still less than 90%, which can be further enhanced by increasing and optimizing N .

2) *Cascaded Multiple Elementary Units*: As previously mentioned, the SBMF was set as $B = 7$ T. The optimal N was then obtained in cascaded multiple elementary units by comparing the transmission and absorption for various values of N . The transmittance, reflectance, and absorption of cascaded multiple

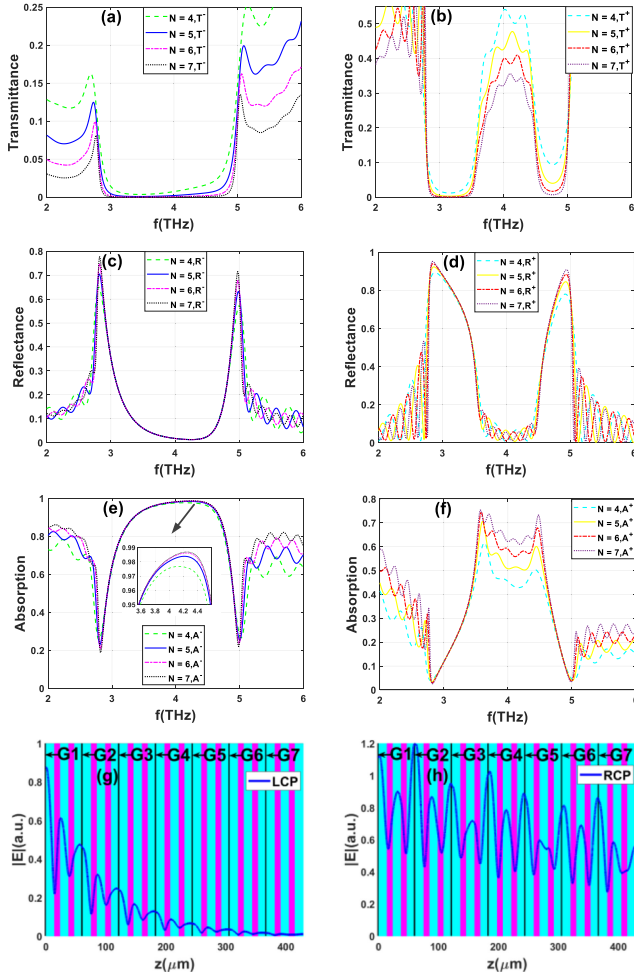


Fig. 6. (a) and (b) Transmittance, (c) and (d) reflectance, and (e) and (f) absorption of cascaded multiple elementary units for the LCP and RCP waves with various N . (g) and (h) Electric field distributions in $(GC(AB)^2)^7$ for $B = 7$ T.

elementary units for the LCP wave are shown in Fig. 6(a), (c), and (e), respectively. With stable reflectance, the transmittance in the photonic band gap (i.e., from 2.95 to 4.7 THz) decreased as N increased when $N \geq 4$. Subsequently, the absorption of the LCP wave increased, as shown in Fig. 6(e). The absorption increased slightly when $N > 5$, which can be attributed to the weak power dissipation in the higher-order elementary units (e.g., 6th and 7th), as indicated in Fig. 6(g). Therefore, N can be optimized to 5 for cascaded multiple elementary units. $(GC(AB)^2)^5$ was able to operate in a broadband range of 3.34 - 4.68 THz with an absorption of $\geq 90\%$ for the LCP wave, as shown in Fig. 6(e). Compared with the LCP wave, the transmittance and reflectance of the RCP wave became higher and narrower, which caused the deteriorated absorption, as shown in Fig. 6(b), (d), (f), and (h).

C. Influence of Model Parameters on the Absorption Performance of Cascaded Quintuple Elementary Units

The absorption performance of $(GC(AB)^2)^5$ can be influenced by the Fermi level (E_F), dielectric loss, and thickness d_s and refractive index n_c of the spacer layer.

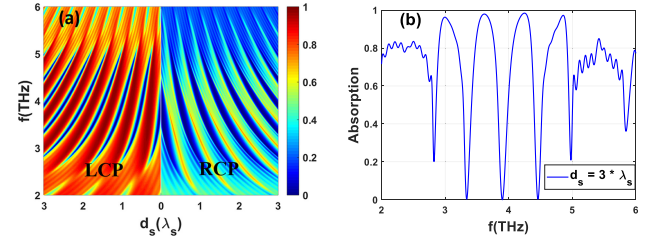


Fig. 7. Frequency / thickness dependent absorption of $(GC(AB)^2)^5$ for $B = 7$ T. (a) LCP and RCP waves ($\lambda_s = \lambda_0/n_D$), and (b) LCP wave at $d_s = 3\lambda_s$.

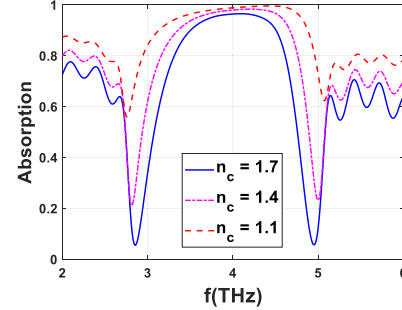


Fig. 8. n_c -dependent absorption of $(GC(AB)^2)^5$ for the LCP wave when $B = 7$ T.

1) *Influence of Thickness d_s* : The absorption peaks for the LCP and RCP waves of the d_s -dependent absorption of $(GC(AB)^2)^5$ exhibited periodicity as d_s increased in the photonic band gap, as shown in Fig. 7(a). In addition, the absorption of the LCP wave was significantly higher than that of the RCP wave. More importantly, there were multiple bands with high absorption in the photonic band gap when $d_s = 3\lambda_s$, which could be utilized to achieve a multi-band THz absorber, as shown in Fig. 7(b).

2) *Influence of Refractive Index n_c* : As the n_c decreased, the absorption performance of the LCP wave improved, as shown in Fig. 8. As the n_c decreased, the difference in the refractive index between the spacer layer and top layer (SiO_2) of the 1DPC increased, which increased the reflected wave in the spacer layer. Subsequently, the light-matter interaction between the reflected wave and graphene were enhanced, which improved the bandwidth and absorption of the LCP wave. To obtain higher absorption performance, n_c should be distanced from the refractive index of the top layer of the 1DPC.

3) *Influence of Fermi Levels E_F* : From (1) and (2), the Fermi level E_F can tune the conductivity of the graphene, which can subsequently influence the absorption of $(GC(AB)^2)^5$, as shown in Fig. 9. The absorption performance of the LCP wave firstly improved and then degraded in the photonic band gap as $|E_F|$ increased. Meanwhile, the performance of the RCP wave exhibited a similar performance. It is noteworthy that the proposed model was optimal for the LCP wave when E_F was in the range of -0.22 to -0.36 eV.

4) *Influence of the Nonmagnetic Dielectric Loss*: As previously mentioned, the dielectric in the proposed model $(GC(AB)^2)^5$ was assumed to be lossless. In practical applications, nonmagnetic dielectrics such as MgF_2 and SiO_2 may

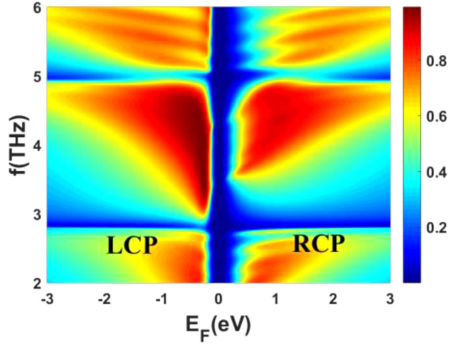


Fig. 9. E_F -dependent absorption of $(GC(AB)^2)^5$ for LCP and RCP waves when $B = 7$ T.

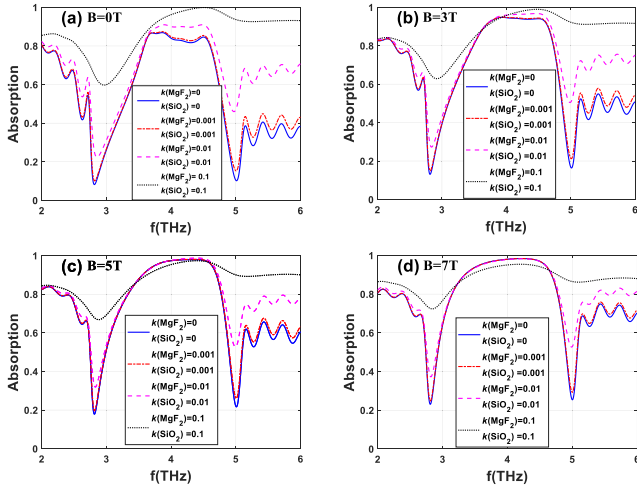


Fig. 10. Absorption of the proposed model $(GC(AB)^2)^5$ for the LCP wave with various extinction coefficients: (a) $B = 0$ T, (b) $B = 3$ T, (c) $B = 5$ T, and (d) $B = 7$ T.

be lossy (i.e., the extinction coefficients $k(\text{MgF}_2)$ and $k(\text{SiO}_2)$ are nonzero), and the loss can affect the absorption performance. The absorption performances of the proposed model with various extinction coefficients ($k(\text{MgF}_2)$ and $k(\text{SiO}_2)$) for $B = 0, 3, 5,$ and 7 T are shown in Fig. 10. The change in the absorption performance difference became less obvious as the SBMF increased. In addition, the absorption performance was almost identical in the photonic band gap when $k \leq 0.01$, which is beneficial for obtaining a stable absorption performance for applications.

IV. CONCLUSION

This study proposed a magnetically tunable THz broadband absorber based on graphene and 1DPC. The absorption performance was investigated using the 4×4 transfer matrix method. Furthermore, the proposed graphene-based 1DPC broadband absorber was dynamically tuned using an SBMF. The proposed absorber could absorb the LCP wave in a broadband range from 3.34 to 4.68 THz with an absorption greater than 90% at $B = 7$ T. In addition, the influence of the thickness and refractive index of the spacer layer, Fermi level, and losses of dielectric

layers on the absorption performance were analyzed. From these analyses, it was observed that a multi-band THz absorber could be achieved for the LCP wave by varying the thickness. The absorption performance of the LCP wave improved by tuning the Fermi level and decreasing the refractive index. Furthermore, the proposed model demonstrated a stable absorption performance when $B = 7$ T and the extinction coefficient of the dielectric layer $k \leq 0.01$, which is beneficial for practical applications. These investigations provide a new concept for the design of magnetically tunable THz broadband absorbers, which have the potential for many applications, such as broadband filters, anti-radar stealth, and sensors.

REFERENCES

- [1] R. R. Nair *et al.*, "Fine structure constant defines visual transparency of graphene," *Science*, vol. 320, no. 5881, pp. 1308–1308, Jun. 2008, doi: [10.1126/Science.1156965](https://doi.org/10.1126/Science.1156965).
- [2] M. M. Jadidi *et al.*, "Nonlinear terahertz absorption of graphene plasmons," *Nano Lett.*, vol. 16, no. 4, pp. 2734–2738, Apr. 2016, doi: [10.1021/acs.nanolett.6b00405](https://doi.org/10.1021/acs.nanolett.6b00405).
- [3] L. Ju *et al.*, "Graphene plasmonics for tunable terahertz metamaterials," *Nat. Nanotechnol.*, vol. 6, no. 10, pp. 630–634, Oct. 2011, doi: [10.1038/NNANO.2011.146](https://doi.org/10.1038/NNANO.2011.146).
- [4] B. Sensale-Rodriguez *et al.*, "Broadband graphene terahertz modulators enabled by intraband transitions," *Nat. Commun.*, vol. 3, Apr. 2012, Art. no. 780, doi: [10.1038/ncomms1787](https://doi.org/10.1038/ncomms1787).
- [5] S. G. Johnson, A. Mekis, S. H. Fan, and J. D. Joannopoulos, "Molding the flow of light," *Comput. Sci. Eng.*, vol. 3, no. 6, pp. 38–47, Nov. 2001, doi: [10.1109/5992.963426](https://doi.org/10.1109/5992.963426).
- [6] E. Yablonovitch, "Inhibited spontaneous emission in solid-state physics and electronics," *Phys. Rev. Lett.*, vol. 58, no. 20, pp. 2059–2062, May 1987.
- [7] S. John, "Strong localization of photons in certain disordered dielectric superlattices," *Phys. Rev. Lett.*, vol. 58, no. 23, pp. 2486–2489, Jun. 1987.
- [8] M. A. Vincenti, D. de Ceglia, M. Grande, A. D'Orazio, and M. Scalora, "Nonlinear control of absorption in one-dimensional photonic crystal with graphene-based defect," *Opt. Lett.*, vol. 38, no. 18, pp. 3550–3553, Sep. 2013, doi: [10.1364/OL.38.003550](https://doi.org/10.1364/OL.38.003550).
- [9] R. Miloua *et al.*, "Peak, multi-peak and broadband absorption in graphene-based one-dimensional photonic crystal," *Opt. Commun.*, vol. 330, pp. 135–139, Nov. 2014, doi: [10.1016/j.optcom.2014.05.043](https://doi.org/10.1016/j.optcom.2014.05.043).
- [10] M. Grande *et al.*, "Absorption and losses in one-dimensional photonic-crystal-based absorbers incorporating graphene," *IEEE Photon. J.*, vol. 6, no. 6, Dec. 2014, Art. no. 0600808, doi: [10.1109/JPHOT.2014.2356495](https://doi.org/10.1109/JPHOT.2014.2356495).
- [11] H. J. Song and T. Nagatsuma, "Present and future of terahertz communications," *IEEE Trans. Terahertz Sci. Technol.*, vol. 1, no. 1, pp. 256–263, Sep. 2011, doi: [10.1109/THZ.2011.2159552](https://doi.org/10.1109/THZ.2011.2159552).
- [12] W. L. Chan, J. Deibel, and D. M. Mittleman, "Imaging with terahertz radiation," *Rep. Prog. Phys.*, vol. 70, no. 8, pp. 1325–1379, Aug. 2007, doi: [10.1088/0034-4885/70/8/R02](https://doi.org/10.1088/0034-4885/70/8/R02).
- [13] P. H. Siegel, "Terahertz technology in biology and medicine," *IEEE Trans. Microw. Theory Techn.*, vol. 52, no. 10, pp. 2438–2447, Oct. 2004, doi: [10.1109/TMTT.2004.835916](https://doi.org/10.1109/TMTT.2004.835916).
- [14] M. Tonouchi, "Cutting-edge terahertz technology," *Nat. Photon.*, vol. 1, no. 2, pp. 97–105, Feb. 2007, doi: [10.1038/nphoton.2007.3](https://doi.org/10.1038/nphoton.2007.3).
- [15] X. Wang, X. Jiang, Q. You, J. Guo, X. Y. Dai, and Y. J. Xiang, "Tunable and multichannel terahertz perfect absorber due to tamm surface plasmons with graphene," *Photon. Res.*, vol. 5, no. 6, pp. 536–542, Dec. 2017, doi: [10.1364/PRJ.5.000536](https://doi.org/10.1364/PRJ.5.000536).
- [16] X. K. Kong, X. Z. Shi, J. J. Mo, Y. T. Fang, X. L. Chen, and S. B. Liu, "Tunable multichannel absorber composed of graphene and doped periodic structures," *Opt. Commun.*, vol. 383, pp. 391–396, Jan. 2017, doi: [10.1016/j.optcom.2016.09.038](https://doi.org/10.1016/j.optcom.2016.09.038).
- [17] Y. Q. Kang and H. M. Liu, "Wideband absorption in one dimensional photonic crystal with graphene-based hyperbolic metamaterials," *Superlattices Microstruct.*, vol. 114, pp. 355–360, Feb. 2018, doi: [10.1016/j.spmi.2017.12.046](https://doi.org/10.1016/j.spmi.2017.12.046).
- [18] H. I. Wang *et al.*, "Reversible photochemical control of doping levels in supported graphene," *J. Phys. Chem. C*, vol. 121, no. 7, pp. 4083–4091, Feb. 2017, doi: [10.1021/acs.jpcc.7b00347](https://doi.org/10.1021/acs.jpcc.7b00347).

- [19] A. Rashidi, A. Namdar, and R. Abdi-Ghaleh, "Magnetically tunable enhanced absorption of circularly polarized light in graphene-based 1D photonic crystals," *Appl. Opt.*, vol. 56, no. 21, pp. 5914–5919, Jul. 2017, doi: [10.1364/AO.56.005914](https://doi.org/10.1364/AO.56.005914).
- [20] W. Pan, X. Yu, J. Zhang, and W. Zeng, "A broadband terahertz metamaterial absorber based on two circular split rings," *IEEE J. Quantum Electron.*, vol. 53, no. 2, Feb. 2017, Art. no. 8500206, doi: [10.1109/JQE.2016.2643279](https://doi.org/10.1109/JQE.2016.2643279).
- [21] A. Ferreira, J. Viana-Gomes, Y. V. Bludov, V. Pereira, N. M. R. Peres, and A. H. Castro Neto, "Faraday effect in graphene enclosed in an optical cavity and the equation of motion method for the study of magneto-optical transport in solids," *Phys. Rev. B*, vol. 84, no. 23, Dec. 2011, Art. no. 235410, doi: [10.1103/PhysRevB.84.235410](https://doi.org/10.1103/PhysRevB.84.235410).
- [22] T. R. Zhan, X. Shi, Y. Y. Dai, X. H. Liu, and J. Zi, "Transfer matrix method for optics in graphene layers," *J. Phys. Condens. Matter*, vol. 25, no. 21, May 2013, Art. no. 215301, doi: [10.1088/0953-8984/25/21/215301](https://doi.org/10.1088/0953-8984/25/21/215301).
- [23] Š. Višňovský, K. Postava, and T. Yamaguchi, "Magneto-optic polar Kerr and Faraday effects in magnetic superlattices," *Czech. J. Phys.*, vol. 51, no. 9, pp. 917–949, Sep. 2001, doi: [10.1023/A:1012300926059](https://doi.org/10.1023/A:1012300926059).
- [24] N. M. R. Peres and Y. V. Bludov, "Enhancing the absorption of graphene in the terahertz range," *EPL*, vol. 101, no. 5, Mar. 2013, Art. no. 58002, doi: [10.1209/0295-5075/101/58002](https://doi.org/10.1209/0295-5075/101/58002).
- [25] T. Xie, D. B. Chen, H. P. Yang, Y. H. Xu, Z. R. Zhang, and J. B. Yang, "Tunable broadband terahertz waveband absorbers based on fractal technology of graphene metamaterial," *Nanomaterials*, vol. 11, no. 2, Feb. 2021, Art. no. 269, doi: [10.3390/nano11020269](https://doi.org/10.3390/nano11020269).
- [26] E. Ataei, M. Sharifian, and N. Z. Bidoki, "Magnetized plasma photonic crystals band gap," *J. Plasma Phys.*, vol. 80, pp. 581–592, Aug. 2014, doi: [10.1017/S0022377814000105](https://doi.org/10.1017/S0022377814000105).
- [27] I. Crassee *et al.*, "Giant Faraday rotation in single- and multi-layer graphene," *Nat. Phys.*, vol. 7, no. 1, pp. 48–51, Jan. 2011, doi: [10.1038/NPHYS1816](https://doi.org/10.1038/NPHYS1816).
- [28] J. T. Liu, N. H. Liu, J. Li, X. J. Li, and J. H. Huang, "Enhanced absorption of graphene with one-dimensional photonic crystal," *Appl. Phys. Lett.*, vol. 101, no. 5, Jul. 2012, Art. no. 052104, doi: [10.1063/1.4740261](https://doi.org/10.1063/1.4740261).
- [29] P. J. Stephens, "Magnetic circular dichroism," *Annu. Rev. Phys. Chem.*, vol. 25, no. 1, pp. 201–232, 1974.
- [30] J. K. S. Poon, J. Scheuer, S. Mookherjea, G. T. Paloczi, Y. Y. Huang, and A. Yariv, "Matrix analysis of microring coupled-resonator optical waveguides," *Opt. Exp.*, vol. 12, no. 1, pp. 90–103, Jan. 2004, doi: [10.1364/OPEX.12.000090](https://doi.org/10.1364/OPEX.12.000090).
- [31] M. Bayindir, S. Tanriseven, and E. Ozbay, "Propagation of light through localized coupled-cavity modes in one-dimensional photonic band-gap structures," *Appl. Phys. A*, vol. 72, no. 1, pp. 117–119, Jan. 2001, doi: [10.1007/s003390000700](https://doi.org/10.1007/s003390000700).